35th Annual International Conference of the IEEE EMBS
Osaka, Japan, 3 - 7 July, 2013

# Rate-equation Approach to Optimal Density Ratio of K-Rb Hybrid Cells for Optically Pumped Atomic Magnetometers*

Yosuke Ito[1], Hiroyuki Ohnishi[2], Keigo Kamada[2], and Tetsuo Kobayashi[2]

***Abstract*— The goal of this study is to determine optimal conditions of optically pumped atomic magnetometers using a hybrid cell of potassium and rubidium atoms. We theoretically investigated the properties of the magnetometers and considered the optimal density ratio of potassium and rubidium atoms. We found that the experimental results agreed well with the theoretical estimations and the density ratio of potassium and rubidium atoms should be around 200 to achieve the highest sensitivity.**

## I. Introduction

In recent years, optically pumped atomic magnetometers (OPAMs) are of scientific and practical interest as the sensors for biomagnetic measurements. Traditionally, superconducting quantum interference devices (SQUIDs) have been widely used for biomagnetic measurements such as magnetoencephalography (MEG) and magnetocardiography (MCG). The SQUIDs have a sufficient sensitivity ($\sim$ 1 fT/Hz$^{1/2}$) for biomagnetic fields, but it is difficult to be downsized and low-cost because they require cryogenic cooling for maintaining the superconducting state. In contract, the OPAMs require no cooling systems because they measure magnetic fields with the atomic spin polarization originated from optical pumping of alkali metal atoms. Furthermore, the theoretical limit of the OPAMs is reported to be 0.01 fT/Hz$^{1/2}$ [1] and the experimentally-achieved sensitivity is 0.16 fT/Hz$^{1/2}$ under the spin-exchange relaxation free (SERF) condition [2]. In addition, previous studied have demonstrated the use of the OPAM in nuclear magnetic resonance (NMR) spectroscopy [3], MCG [4], and MEG [5].

We have investigated the OPAM using a hybrid cell of potassium and rubidium atoms since it can suppress the noise caused by deexcitation lights from the sensing atoms [6]. With the OPAM, we have measured human MCG successfully [7]. To improve the sensitivity of the OPAM for human MEG measurements, the density ratio of potassium and rubidium atoms is essential, so that we theoretically investigate the optimal density ratio for high output signals by the rate-equation approach in this paper.

*This work was supported in part by the Innovative Techno-Hub for Integrated Medical Bio-imaging of the Project for Developing Innovation Systems, and a Grant-in-Aid for Scientific Research (24240081) both from the Ministry of Education, Culture, Sports, Science, and Technology (MEXT), Japan.

[1]Y. Ito is with Advanced Biomedical Engineering Research Unit, Center for the Promotion of Interdisciplinary Education and Research, Kyoto University, KyotoDaigakuKatsura, Nishikyo-ku, Kyoto 615-8510,Japan (corresponding author to provide phone: +81-75-383-2259; fax: +81-75-383-2259; e-mail: yito@kuee.kyoto-u.ac.jp)

[2]H. Ohnishi, K. Kamada, and T. Kobayashi are with the Department of Electrical Engineering, Kyoto University, KyotoDaigakuKatsura, Nishikyo-ku, Kyoto 615-8510, Japan

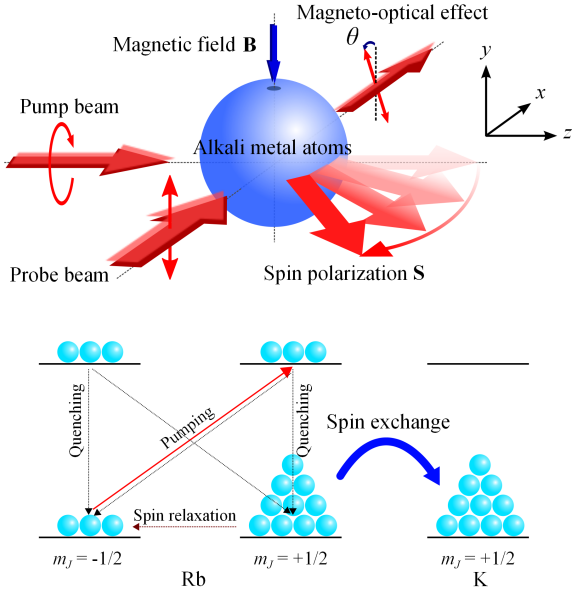


Figure 1. Principle of OPAMs (upper) and spin polarization transfer from rubidium to potassium atoms by spin-exchange collisions (lower).

## II. Theory

### A. Principle of operation

Fig. 1 shows the principle of the OPAMs using a hybrid cell of potassium and rubidium atoms. In the present study, we consider optically-pumped rubidium and probed potassium atoms due to smaller spin-destruction cross section of potassium atoms [1], [8]. The circularly polarized pump beam, which has the frequency corresponding to the resonant frequency of rubidium atoms and penetrates along $z$ direction, causes the spin polarization of the rubidium atoms $\mathbf{S}^{\mathrm{Rb}} = S_z^{\mathrm{Rb}}\hat{\mathbf{z}}$. Then the spin transfers to the potassium atoms via spin-exchange collisions between rubidium and potassium atoms, so that the spin polarization of potassium atoms $\mathbf{S}^{\mathrm{K}} = S_z^{\mathrm{k}}\hat{\mathbf{z}}$ arises [9].

When a magnetic field $\mathbf{B} = B_y\hat{\mathbf{y}}$ is applied, the spin polarization precess around $y$ direction by the torque $\mathbf{S} \times \mathbf{B}$ [10]. $S_x$, which is the $x$ component of $\mathbf{S}$, causes the magneto-optical effect to the linearly polarized probe beam penetrating from $x$ direction, that is, the polarization plane of the probe beam is rotated. Measuring the rotation angle by a polarimeter, we can obtain $B_y$ as a voltage value. Furthermore, by applying a bias magnetic field along $z$ direction $B_0$, $\mathbf{S}$ precess along the bias field and the OPAM is sensitive to the magnetic field whose frequency is around

$f_0 = \omega_0/2\pi = \gamma B_0/2\pi$, where $\gamma$ is the gyromagnetic ratio.

The output signal $S_{\rm out}$ of the OPAM is described by the following expressions [11], [12]:

$$S_{\rm out} = \eta I_{\rm probe} e^{\alpha l} \sin(2\theta), \quad (1)$$

$$\alpha = n_{\rm K} c r_{\rm e} f \frac{\Gamma/2}{(\nu_{\rm probe}-\nu_0)^2 + (\Gamma/2)^2}, \quad (2)$$

$$\theta = \frac{1}{2} n_{\rm K} c r_{\rm e} f \frac{\nu_{\rm probe}-\nu_0}{(\nu_{\rm probe}-\nu_0)^2 + (\Gamma/2)^2} l S_x, \quad (3)$$

where $\eta$ is the conversion efficiency from the probe beam power to output voltage, $I_{\rm probe}$ is the intensity of the probe beam, $\alpha$ is the attenuation constant of the probe beam, $l$ is the dimension of the cross region of the pump and probe beams along $x$ direction, and $\theta$ is the magneto-optical rotation angle. $\nu_{\rm probe}$ is the frequency of the probe beam, $\nu_0$ is the resonant frequency of potassium, $n_{\rm K}$ is the density of the potassium atoms, $c$ is the light velocity, and $r_{\rm e}$ is the classical electron radius. $f$ is the oscillator strength and the value is about 1/3 for the D1 transition. $\Gamma$ is the linewidth of the pressure-broadened optical absorption caused by buffer gases such as helium and nitrogen used for quenching and to slow down the diffusion of alkali metal atoms.

### *B. Model*

Considering (1), (2), and (3), the unknown is only $S_x$, so that we now calculate $S_x$ by the rate-equation approach and Bloch equations.

First, we think about the equilibrium state of spin polarization under zero field condition. Each alkali metal atom has the electron spin $\pm 1/2$. Let us designate by $\uparrow$ and $\downarrow$ the electron spin $+1/2$ and $-1/2$, respectively. By this notation, for instance, we can describe the spin-exchange collision between a rubidium atom whose spin is $+1/2$ and a potassium atom whose spin is $-1/2$ as follows:

$$\mathrm{Rb}(\uparrow) + \mathrm{K}(\downarrow) \xrightarrow{k_{\rm SE}} \mathrm{Rb}(\downarrow) + \mathrm{K}(\uparrow), \quad (4)$$

where $k_{\rm SE}$ is the rate coefficient of the spin-exchange collision between potassium and rubidium atoms.

The reaction set for this study is shown in Table I. $\overline{v}$ is their average relative velocity. Under high pressure condition, we need to think about three-body collisions. However, there are not sufficient data, so that such collisions are not considered in this calculation as the first step of the study. In addition, the rate coefficients of the collisions between different kinds of alkali metal atoms are unknown. Here, we introduce a drastic assumption of $k_{\rm SE} = k_{\rm SE(K,K)}$ because the values of $k_{\rm SE(K,K)}$ and $k_{\rm SE(Rb,Rb)}$ are quite similar. On the other hand, $k_{\rm SD(Rb,Rb)}$ is 9 times larger than $k_{\rm SD(K,K)}$, so that $k_{\rm SD(K,Rb)}$ and $k_{\rm SD(Rb,K)}$ should be treated carefully. Meanwhile, in this study, we assume $k_{\rm SD(K,Rb)} = k_{\rm SD(Rb,K)} = k_{\rm SD(K,K)}$ because the calculated results are similar even if we select the value of $k_{\rm SD(Rb,Rb)}$ as $k_{\rm SD(K,Rb)}$ and $k_{\rm SD(Rb,K)}$. With these assumptions, the dominant equation of the density of $n_{\rm K}(\uparrow)$ is expressed by the following equation:

$$\begin{aligned}\frac{d}{dt} n_{\rm K}(\uparrow) &= k_{\rm SE} n_{\rm Rb}(\uparrow) n_{\rm K}(\downarrow) - k_{\rm SE} n_{\rm Rb}(\downarrow) n_{\rm K}(\uparrow) \\ &\quad - X^{\rm K}_{\rm SD}\left[n_{\rm K}(\uparrow) - n_{\rm K}(\downarrow)\right] - X^{\rm K}_{\rm Wall}\left[n_{\rm K}(\uparrow) - n_{\rm K}(\downarrow)\right], \\ X^{\rm K}_{\rm SD} &= k_{\rm SD(K,K)} n_{\rm K} + k_{\rm SD(K,Rb)} n_{\rm Rb} \\ &\quad + k_{\rm SD(K,N_2)} n_{\rm N_2} + k_{\rm SD(K,He)} n_{\rm He}, \\ X^{\rm K}_{\rm Wall} &= D\left(\frac{\pi}{R}\right)^2. \end{aligned} \quad (5)$$

Here $X^{\rm K}_{\rm Wall}$ is the wall collision rate and $D$ is the diffusion coefficient. For simplicity, we approximated that the cell was a sphere whose radius was $R$.

Since $n_{\rm K}$ is constant, the time variation of $n_{\rm K}(\downarrow)$ is written by

$$\frac{d}{dt} n_{\rm K}(\downarrow) = -\frac{d}{dt} n_{\rm K}(\uparrow). \quad (6)$$

Here, let us designate by $S^{\rm K}_0$ and $S^{\rm Rb}_0$ the spin polarization of the potassium and rubidium atoms under zero field condition, respectively. $S^{\rm K}_0$ and $S^{\rm Rb}_0$ are defined by the expressions below:

$$S^{\rm K}_0 = \frac{1}{2}\frac{n_{\rm K}(\uparrow) - n_{\rm K}(\downarrow)}{n_{\rm K}}, \quad S^{\rm Rb}_0 = \frac{1}{2}\frac{n_{\rm Rb}(\uparrow) - n_{\rm Rb}(\downarrow)}{n_{\rm Rb}}. \quad (7)$$

By combining (5), (6), and (7), we obtain the following expression:

$$\begin{aligned}\frac{d}{dt} S^{\rm K}_0 &= k_{\rm SE} n_{\rm Rb} S^{\rm Rb}_0 \\ &\quad - \left(R^{\rm K}_{\rm SEP} + R^{\rm K}_{\rm SE} + R^{\rm K}_{\rm SD} + R^{\rm K}_{\rm Wall}\right) S^{\rm K}_0, \end{aligned} \quad (8)$$

where $R^{\rm K}_{\rm SEP} = k_{\rm SE} n_{\rm Rb}(\uparrow)$ is the polarizing rate by the spin-exchange collisions, $R^{\rm K}_{\rm SE} = k_{\rm SE} n_{\rm Rb}(\downarrow)$ is the spin relaxation rate by the spin-exchange collisions, $R^{\rm K}_{\rm SD} = 2X^{\rm K}_{\rm SD}$ is the spin relaxation rate by the spin-destruction collisions, and $R^{\rm K}_{\rm Wall} = 2X^{\rm K}_{\rm Wall}$ is the spin relaxation rate by the wall collisions. In the same manner, we can also obtain the following equation:

$$\begin{aligned}\frac{d}{dt} S^{\rm Rb}_0 &= \frac{R_{\rm OP}}{2} + k_{\rm SE} n_{\rm K} S^{\rm K}_0 \\ &\quad - \left(R_{\rm OP} + R^{\rm Rb}_{\rm SEP} + R^{\rm Rb}_{\rm SE} + R^{\rm Rb}_{\rm SD} + R^{\rm Rb}_{\rm Wall}\right) S^{\rm Rb}_0. \end{aligned} \quad (9)$$

Here, $R_{\rm OP}$ is the optical pumping rate by the pump beam and described by

$$R_{\rm OP} = \frac{2 c r_{\rm e} f I_{\rm pump}}{A_{\rm pump} h \nu^{\rm Rb}_0 \Gamma}, \quad (10)$$

where $I_{\rm pump}$ and $A_{\rm pump}$ are the intensity and the cross section of the pump beam, respectively. $\nu^{\rm Rb}_0$ is the resonant frequency of rubidium atoms.

Solving (8) and (9), $S^{\rm K}_0$ and $S^{\rm Rb}_0$ converge after about 10 $\mu$s in the pump beam power density range 0.01 - 10 mW/cm$^2$,

TABLE I

BASIC COLLISION SET FOR THE HYBRID CELL

| Reaction | Rate Coefficient ($cm^3/s$) | Reference |
|---|---|---|
| *Spin Exchange Collisions* | | |
| $K(\uparrow) + K(\downarrow) \rightarrow K(\downarrow) + K(\uparrow)$ | $k_{SE(K,K)} = 1.8 \times 10^{-14}\overline{v}$ | [13] |
| $Rb(\uparrow) + Rb(\downarrow) \rightarrow Rb(\downarrow) + Rb(\uparrow)$ | $k_{SE(Rb,Rb)} = 1.8 \times 10^{-14}\overline{v}$ | [13] |
| $Rb(\uparrow) + K(\downarrow) \rightarrow Rb(\downarrow) + K(\uparrow)$ | $k_{SE}$ | |
| $Rb(\downarrow) + K(\uparrow) \rightarrow Rb(\uparrow) + K(\downarrow)$ | $k_{SE}$ | |
| *Spin Destruction Collisions*† | | |
| $K(\uparrow) + K \rightarrow K(\downarrow) + K$ | $k_{SD(K,K)} = 1.0 \times 10^{-18}\overline{v}$ | [8] |
| $K(\uparrow) + Rb \rightarrow K(\downarrow) + Rb$ | $k_{SD(K,Rb)}$ | |
| $K(\uparrow) + N_2 \rightarrow K(\downarrow) + N_2$ | $k_{SD(K,N_2)} = 7.9 \times 10^{-23}\overline{v}$ | [8] |
| $K(\uparrow) + He \rightarrow K(\downarrow) + He$ | $k_{SD(K,He)} = 8.0 \times 10^{-25}\overline{v}$ | [14] |
| $Rb(\uparrow) + K \rightarrow Rb(\downarrow) + K$ | $k_{SD(Rb,K)}$ | |
| $Rb(\uparrow) + Rb \rightarrow Rb(\downarrow) + Rb$ | $k_{SD(Rb,Rb)} = 9 \times 10^{-18}\overline{v}$ | [1] |
| $Rb(\uparrow) + N_2 \rightarrow Rb(\downarrow) + N_2$ | $k_{SD(Rb,N_2)} = 1 \times 10^{-22}\overline{v}$ | [1] |
| $Rb(\uparrow) + He \rightarrow Rb(\downarrow) + He$ | $k_{SD(Rb,He)} = 9 \times 10^{-24}\overline{v}$ | [1] |

†We also consider the collisions of $K(\downarrow)$ and $Rb(\downarrow)$ against K, Rb, He, and $N_2$.

and the values are expressed by

$$S_0^{Rb} = \frac{1}{2}\left(R_{SE(all)}^{K} + R_{Rel}^{K}\right) R_{OP} \left[\left(R_{SE(all)}^{K} + R_{Rel}^{K}\right) R_{OP} + R_{SE(all)}^{Rb} R_{Rel}^{K} + R_{SE(all)}^{K} R_{Rel}^{Rb} + R_{Rel}^{K} R_{Rel}^{Rb}\right]^{-1}, \quad (11)$$

$$S_0^{K} = \frac{1}{2} R_{SE(all)}^{K} R_{OP} \left[\left(R_{SE(all)}^{K} + R_{Rel}^{K}\right) R_{OP} + R_{SE(all)}^{Rb} R_{Rel}^{K} + R_{SE(all)}^{K} R_{Rel}^{Rb} + R_{Rel}^{K} R_{Rel}^{Rb}\right]^{-1}, \quad (12)$$

$$R_{SE(all)}^{K} = R_{SEP}^{K} + R_{SE}^{K} = k_{SE} n_{Rb},$$
$$R_{SE(all)}^{Rb} = R_{SEP}^{Rb} + R_{SE}^{Rb} = k_{SE} n_{K},$$
$$R_{Rel}^{K} = R_{SD}^{K} + R_{Wall}^{K}, \quad R_{Rel}^{Rb} = R_{SD}^{Rb} + R_{Wall}^{Rb}.$$

Next, we solve the Bloch equations for the spin polarization of potassium and rubidium atoms when $\mathbf{B} = B' \cos(\omega t)\hat{\mathbf{y}}$ is applied. In this case, the spin polarization vectors of rubidium and potassium are described by the following Bloch equations:

$$\frac{d}{dt}\mathbf{S}^{Rb} = \gamma \mathbf{S}^{Rb} \times \mathbf{B} + \frac{1}{q^{Rb}} \frac{R_{OP}}{2} \hat{\mathbf{z}} + \frac{1}{q^{Rb}} \frac{R_{SEP}^{Rb}}{2} \frac{\mathbf{S}^{K}}{|\mathbf{S}^{K}|} - \left[\frac{1}{q^{Rb}}\left(R_{OP} + R_{SD}^{Rb} + R_{SE(all)}^{Rb}\right) + R_{Wall}^{Rb}\right] \mathbf{S}^{Rb}, \quad (13)$$

$$\frac{d}{dt}\mathbf{S}^{K} = \gamma \mathbf{S}^{K} \times \mathbf{B} + \frac{1}{q^{K}} \frac{R_{SEP}^{K}}{2} \frac{\mathbf{S}^{Rb}}{|\mathbf{S}^{Rb}|} - \left[\frac{1}{q^{K}}\left(R_{SD}^{K} + R_{SE(all)}^{K}\right) + R_{Wall}^{K}\right] \mathbf{S}^{K}, \quad (14)$$

where $q^{Rb}$ and $q^{K}$ are the nuclear slowing-down factor of the rubidium and the potassium atoms, respectively. Under the SERF condition, we can ignore the terms of the spin-exchage collisions between the same kinds of alkali metal atoms.

Here, since the rotation angle of the spin polarization is quite small, we can approximate $S_z^{Rb} \approx S_0^{Rb}$ and $S_z^{K} \approx S_0^{K}$. With this assumption, we can obtain the $x$ components of $\mathbf{S}^{Rb}$ and $\mathbf{S}^{K}$.

## III. METHODS

The hybrid cell consists of a 30-mm cubic glass cell within which potassium and rubidium atoms are enclosed with helium and nitrogen as buffer gases at a ratio of 10:1 at a total pressure of 150 kPa at room temperature. The cell is heated to 453 K to vaporize the alkali metal atoms. Table II shows the list of the hybrid cells, which we calculated and examined the output signals. In this study, the densities of potassium atoms are quite similar and those of rubidium atoms vary drastically at 453 K.

TABLE II

HYBRID CELL CONDITIONS USED IN CALCULATIONS AND EXPERIMENTS.

| K/Rb | K density ($cm^{-3}$) | Rb density ($cm^{-3}$) |
|---|---|---|
| $> 1000$ | $2.0 \times 10^{13}$ | N.D.† |
| 146 | $1.9 \times 10^{13}$ | $1.3 \times 10^{11}$ |
| 16.5 | $1.5 \times 10^{13}$ | $9.1 \times 10^{11}$ |

†We measured the density by laser absorption and the detection limit was $10^{10}$ $cm^{-3}$ order.

In the experiment, as technique similar to the previous one [6] was used, only the main points are shown here. We applied a sinusoidal signal of 34 $pT_{rms}$ and 100 Hz as the test signal. The OPAM was tuned to a resonant frequency of 100 Hz by the bias field. The wavelength of the probe beam was slightly detuned from the D1 resonant wavelength of potassium atoms, i.e., 769.97 nm and its power density is 8 $mW/cm^2$, whereas the wavelength of the pump beam was tuned to the D1 resonant wavelength of rubidium atoms, i.e., 794.97 nm and its power density was varied from 0.01 to 20 $mW/cm^2$ to investigate the output signal dependent on the pump beam power density.

## IV. RESULTS AND DISCUSSION

Fig. 2 shows the calculated and measured output signals as a function of the pump beam power density. The measured values are in good agreement with the calculated ones. In the pump beam power density range 0.01 to 20 $mW/cm^2$, the signal intensities of all hybrid cells increase with an increase in the pump beam power density. In the low pump beam power density region, there is slight difference between calculated and measured values. This is because our model does not include the attenuation of the pump beam power during the propagation in the rubidium gas. Although the

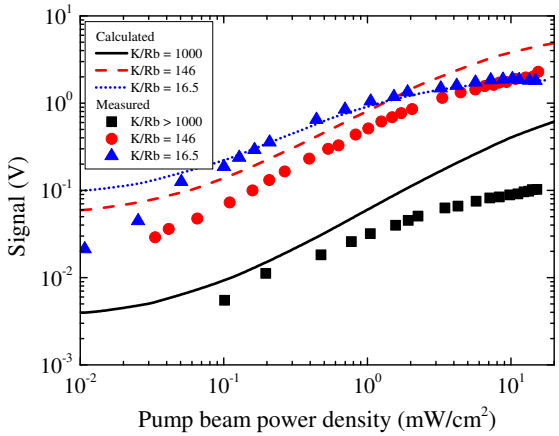


Figure 2. Calculated and measured output signal of OPAM as a function of pump beam power density.

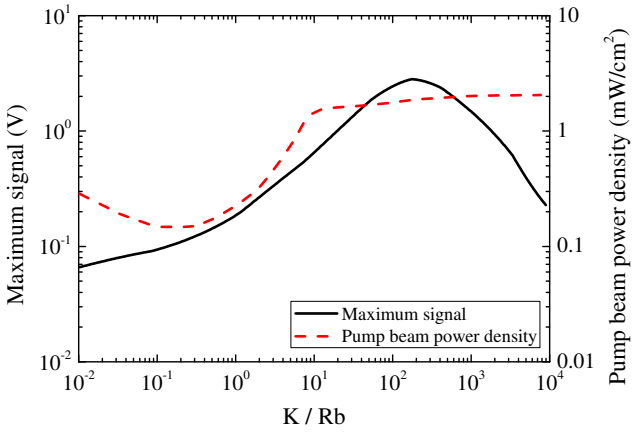


Figure 3. Calculated maximum signals of OPAM as a function of the ratio of densities of potassium and rubidium atoms and required pump beam power density to obtain the maximum signals.

density of the rubidium atoms is small, the pump beam is absorbed by the atoms and it is particularly prominent for the low power pump beam. This effect influences the higher pump beam power density region. The measured values of the cells of $\mathrm{K/Rb} > 1000$ and $\mathrm{K/Rb} = 146$ show slightly negative deviations from the calculated results. It seems that this is also caused by the effect. The higher rubidium density is, the more the photons are absorbed by the atoms. Therefore our model requires to be improved by including the photon absorption.

Estimating noise level of the OPAM, the lowest noise level was 25 $\mathrm{fT_{rms}/Hz^{1/2}}$. This value did not reach those reported by Romalis group [1], [2]. However, they use the modulation technique and the gradiometric measurements to reduce the noise level. These may improve sensitivity of our sensor drastically.

Fig. 3 provides the calculated maximum output signals of the OPAM as a function of the ratio of the densities of the potassium and rubidium atoms. We also display the required pump beam power density to obtain the maximum values. Fig. 3 indicates that we can obtain the maximum signal at around $\mathrm{K/Rb} = 200$ with the pump beam power density of about 20 mW/cm$^2$. The required power density has a minimum at $\mathrm{K/Rb} \approx 0.2$ in a fine balance of the spin-exchange polarization and the spin relaxation by the spin-exchange collisions. Then, as increasing K/Rb, the power density increases gradually up to $\mathrm{K/Rb} \approx 10$, above which it approaches a constant value. This can be explained by (11) and (12). In the case of sufficiently-large pump beam power density, i.e., much high $R_{\mathrm{OP}}$, $S_0^{\mathrm{Rb}}$ approaches 1/2. Under this condition, $S_0^{\mathrm{K}} \approx 0$ for the case of small $n_{\mathrm{Rb}}$. Consequently, the maximum signal diminishes with an increase in K/Rb.

From above consideration, it is conjectured that the optimal K/Rb in a hybrid cell for the high output signal is estimated to be around 200.

## V. Conclusions

The optimal density ratio of potassium and rubidium atoms was investigated by the rate-equation approach. The experimental and calculated values showed good agreement. Using the approach, we estimated the optimal density ratio of potassium and rubidium atoms K/Rb was 200 for the high output signal. In the future, we plan to expand our model to include the three-body collisions and the photon absorption, fabricate the hybrid cell with $\mathrm{K/Rb} \approx 200$, and measure human MEGs with the OPAM using the hybrid cell.

## References


[1] J. C. Allred, R. N. Lyman, T. W. Kornack, and M. V. Romalis, "High-sensitivity atomic magnetometer unaffected by spin-exchange relaxation," *Phys. Rev. Lett.*, vol. 89, no. 13, p. 130801, 2002.

[2] H. B. Dang, A. C. Maloof, and M. V. Romalis, "Ultrahigh sensitivity magnetic field and magnetization measurements with an atomic magnetometer," *Appl. Phys. Lett.*, vol. 97, no. 15, p. 151110, 2010.

[3] I. M. Savukov, S. J. Seltzer, and M. V. Romalis, "Detection of nmr signals with a radio-frequency atomic magnetometer," *J. Magn. Res.*, vol. 185, no. 2, p. 214, 2007.

[4] G. Bison, R. Wynands, and A. Weis, "A laser-pumped magnetometer for the mapping of human cardiomagnetic fields," *Appl. Phys. B: Lasers Opt.*, vol. 76, p. 325, 2003, 10.1007/s00340-003-1120-z.

[5] D. Budker and M. Romalis, "Optical magnetometry," *Nat. Phys.*, vol. 3, p. 227, 2007.

[6] Y. Ito, H. Ohnishi, K. Kamada, and T. Kobayashi, "Sensitivity improvement of spin-exchange relaxation free atomic magnetometers by hybrid optical pumping of potassium and rubidium," *IEEE Trans. Magn.*, vol. 47, no. 10, p. 3550, 2011.

[7] ——, "Development of an optically pumped atomic magnetometer using a K-Rb hybrid cell and its application to magnetocardiography," *AIP Advances*, vol. 2, no. 3, p. 032127, 2012.

[8] S. Kadlecek, L. W. Anderson, and T. Walker, "Measurement of potassium-potassium spin relaxation cross sections," *Nucl. Instrum. Meth. Phys. Res. A*, vol. 402, no. 2-3, p. 208, 1998.

[9] H. G. Dehmelt, "Spin resonance of free electrons polarized by exchange collisions," *Phys. Rev.*, vol. 109, no. 2, p. 381, 1958.

[10] D. Suter, *The physics of laser-atoms interactions*. Cambridge University Press, 1997, pp. 187–171.

[11] S. Appelt, A. B.-A. Baranga, C. J. Erickson, M. V. Romalis, A. R. Young, and W. Happer, "Theory of spin-exchange optical pumping of $^3$He and $^{129}$Xe," *Phys. Rev. A*, vol. 58, no. 2, p. 1412, 1998.

[12] I. M. Savukov, S. J. Seltzer, M. V. Romalis, and K. L. Sauer, "Tunable atomic magnetometer for detection of radio-frequency magnetic fields," *Phys. Rev. Lett.*, vol. 95, no. 6, p. 063004, 2005.

[13] N. W. Ressler, R. H. Sands, and T. E. Stark, "Measurement of spin-exchange cross sections for $\mathrm{Cs^{133}}$, $\mathrm{Rb^{87}}$ $\mathrm{Rb^{85}}$, $\mathrm{K^{39}}$, and $\mathrm{Na^{23}}$," *Phys. Rev.*, vol. 184, no. 1, p. 102, 1969.

[14] F. A. Franz and C. Volk, "Electronic spin relaxation of the $4^2S_{1/2}$ state of K induced by K-He and K-Ne collisions," *Phys. Rev. A*, vol. 26, no. 1, p. 85, 1982.